PNAS
www.pnas.org

Supplementary Information for

Skin-resident dendritic cells mediate postoperative pain via CCR4 on sensory neurons

Jaqueline Raymondi Silva[1,2], Mircea Iftinca[3], Francisco Isaac Fernandes Gomes[4], Julia Paige Segal[1], Olivia Margery Anne Smith[1], Courtney Ann Bannerman[1], Atlante Silva Mendes[4], Manon Defaye[3], Madeline Elizabeth. C. Robinson[1], Ian Gilron[1,2,5,6], Thiago Mattar Cunha[4], Christophe Altier[3], and Nader Ghasemlou[1,2,5*]

[1]Department of Biomedical and Molecular Sciences, [2]Department of Anesthesiology and Perioperative Medicine, Queen's University, Kingston, Ontario, Canada; [3]Department of Physiology and Pharmacology, Snyder Institute for Chronic diseases, Cumming school of medicine, University of Calgary, Calgary, Alberta, Canada; [4] Center for Research in Inflammatory Diseases (CRID), Department of Pharmacology, Ribeirão Preto Medical School, University of São Paulo, Brazil; [5]Centre for Neuroscience Studies, [6]School of Policy Studies, Queen's University, Kingston, Ontario, Canada

***Corresponding author:**
Nader Ghasemlou, Ph.D.
Queen's University
Botterell Hall, 18 Stuart St, Rm 754
Kingston, Ontario, Canada, K7L 3N6
Email: nader.ghasemlou@queensu.ca
Phone: 613.533.6854

This PDF file includes:

Figures S1 to S12
Supplementary text
SI References

Supplementary Figures

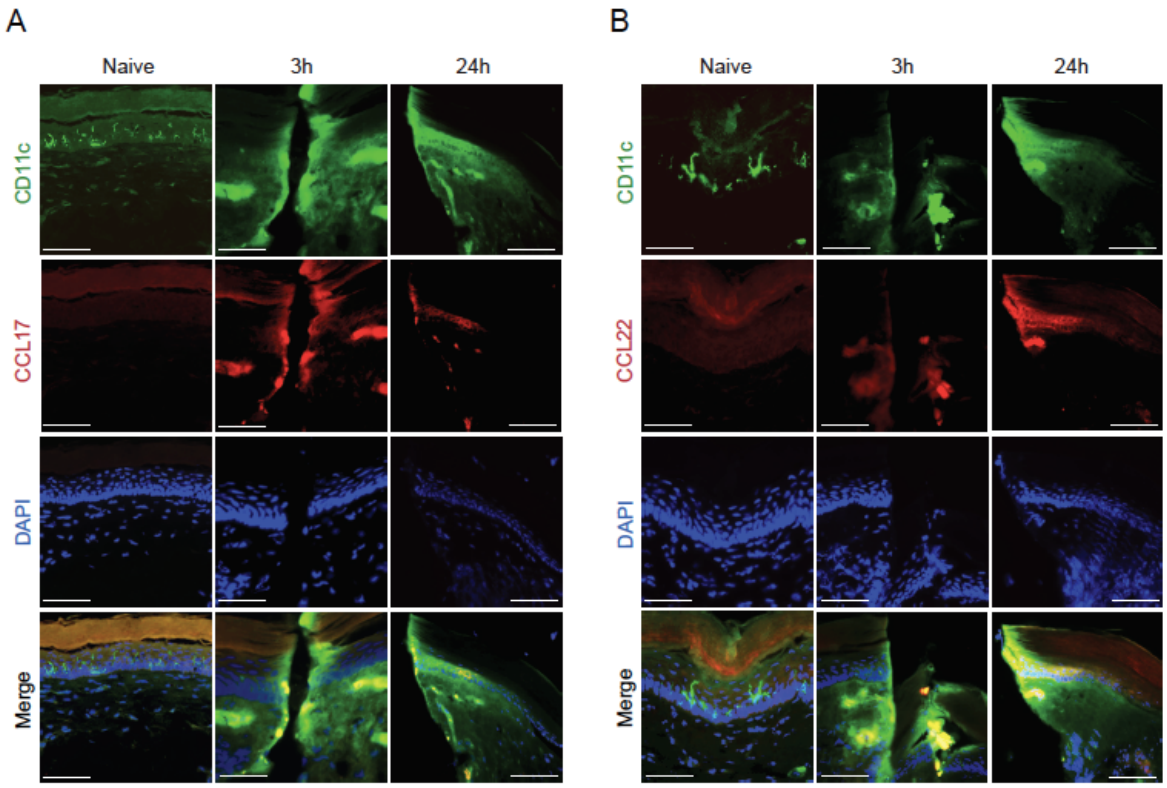

Fig. S1. CCL17 and CCL22 are expressed by CD11c$^+$ dendritic cells after injury
Immunofluorescence analysis of paw sections from naïve and injured mice (3h and 24h) revealed the colocalization of both CCL17 (A) and CCL22 (B) in CD11$^+$ dendritic cells at the site of injury, at both 3 and 24h after incision. There is no expression of either chemokine in uninjured skin. The single stains panels are shown for each staining. Scale bar = 50 µm. Data are representative of 2 experiments.

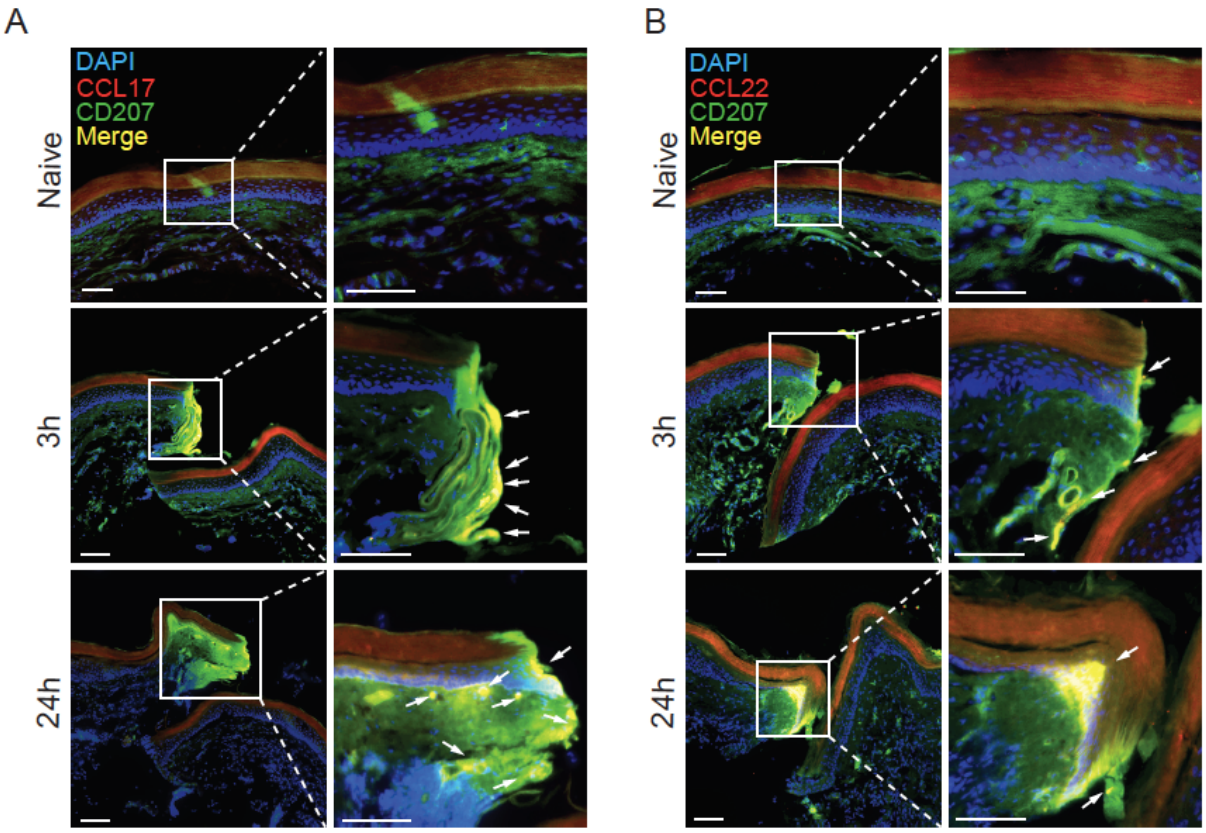

Fig. S2. CCL17 and CCL22 are expressed by Langerhans cells after injury

Immunofluorescence analysis of paw sections from naïve and injured mice (3h and 24h) revealed the colocalization of both CCL17 (A) and CCL22 (B) in $CD207^{+}$ dendritic cells at the site of injury, at both 3 and 24h after incision; insets show high-magnification images at the site of incision. There is no expression of either chemokine in uninjured skin. Arrows point to immunopositive dendritic cells. Scale bar = 50 μm. Data are representative of 2 experiments.

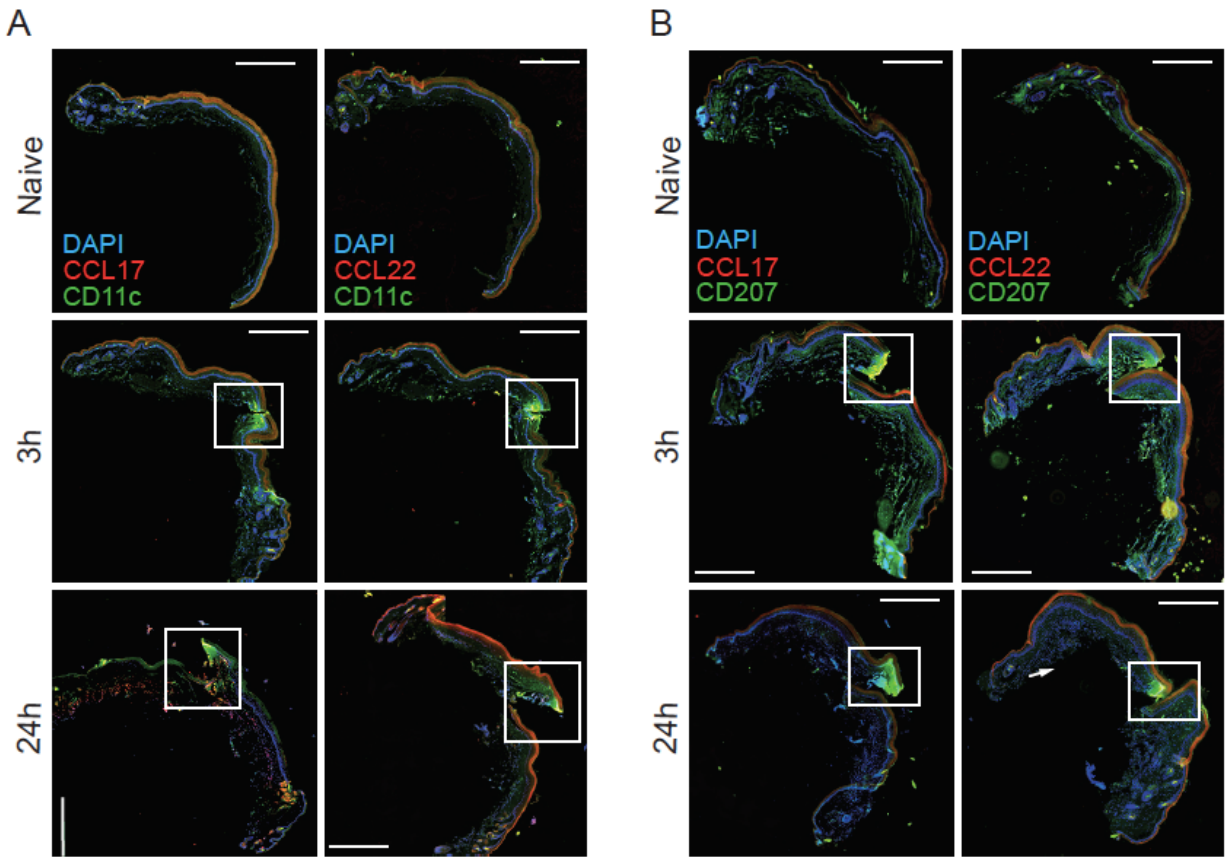

Fig. S3. CCL17 and CCL22 are only expressed at the injury site

Immunofluorescence images of whole paw sections from naïve and injured CD11c-GFP (A) and CD207 GFP mice (B) at 3h and 24h post-surgery. The sections were stained with anti-CCL17 and anti-CCL22. The frames point to the lesion site. Data are representative of 2 (a and b) experiments.

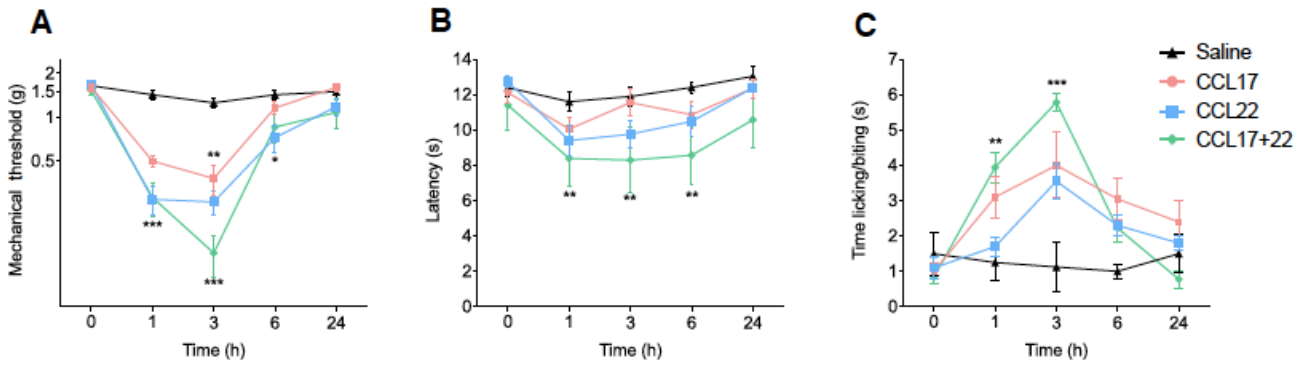

Fig. S4. CCL17 and CCL22 do not show an additive effect

C57BL/6 male mice received an intraplantar injection of a combination of CCL17 and CCL22 (30nM). Mechanical (a), heat (b) and cold (c) hypersensitivity of treated mice, compared to saline mice. Data is represented as mean±SEM; all data analyzed using two-way ANOVA with *post-hoc* Bonferroni test (*P<0.05, **P<0.01, and ***P<0.001). Data are representative of at least n=2 experiments.

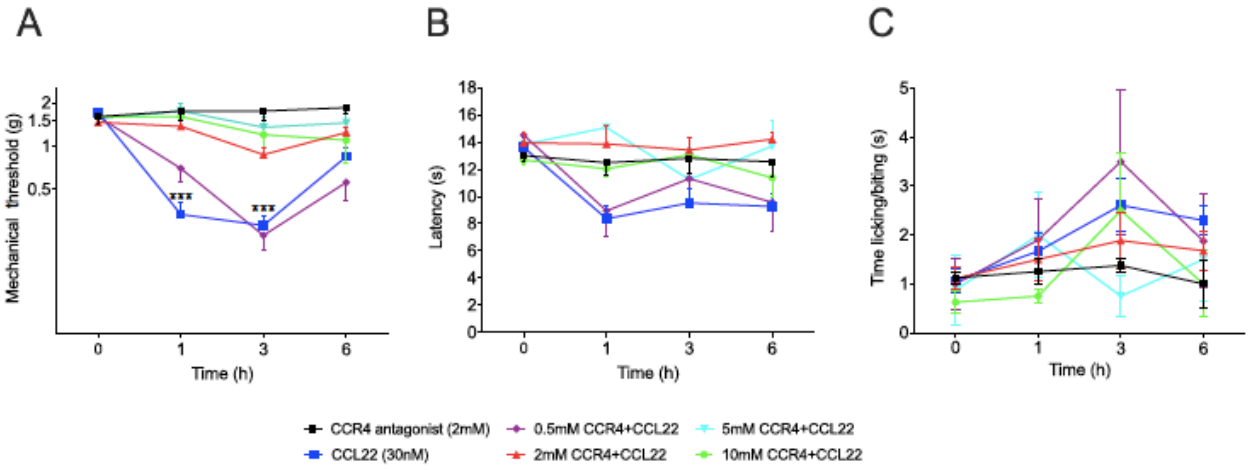

Fig. S5. Dose response treatment with CCR4 antagonist

C57BL/6 male mice received an intraplantar injection of 30nM of CCL22 only, a combination of 30nM of CCL22 and 0.5, 2, 5 and 10 mM of C021 or 2mM of C021 only. Mechanical (A), heat (B) and cold (C) hypersensitivity of mice that received C021 treatment compared to CCL22 treated mice. Data is represented as mean±SEM. Data are representative of at least n=2 experiments.

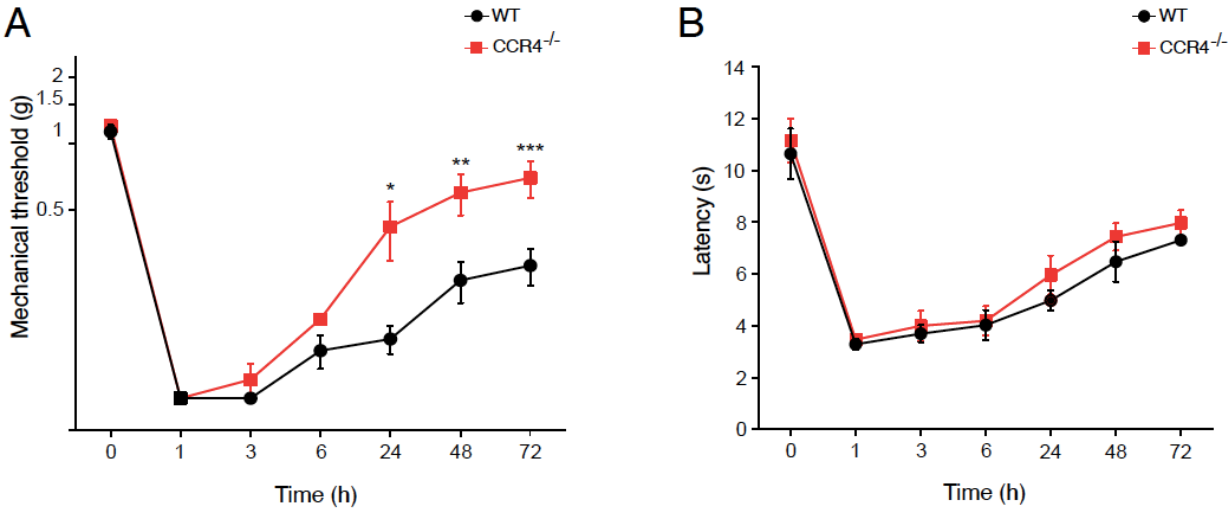

Fig. S6. CCR4 deletion results in attenuated inflammatory pain responses

(A) Mechanical hypersensitivity was significantly reduced in CCR4$^{-/-}$ animals, relative to wild type (WT) controls after incisional wound. (B) Thermal hypersensitivity was not affected by absence of CCR4 expression, with CCR4$^{-/-}$ showing similar responses as WT mice. Data are represented as mean±SEM; all data analyzed using two-way ANOVA with *post-hoc* Bonferroni test (*P<0.05, **P<0.01, and ***P<0.001). Data are representative of at least n=2 experiments.

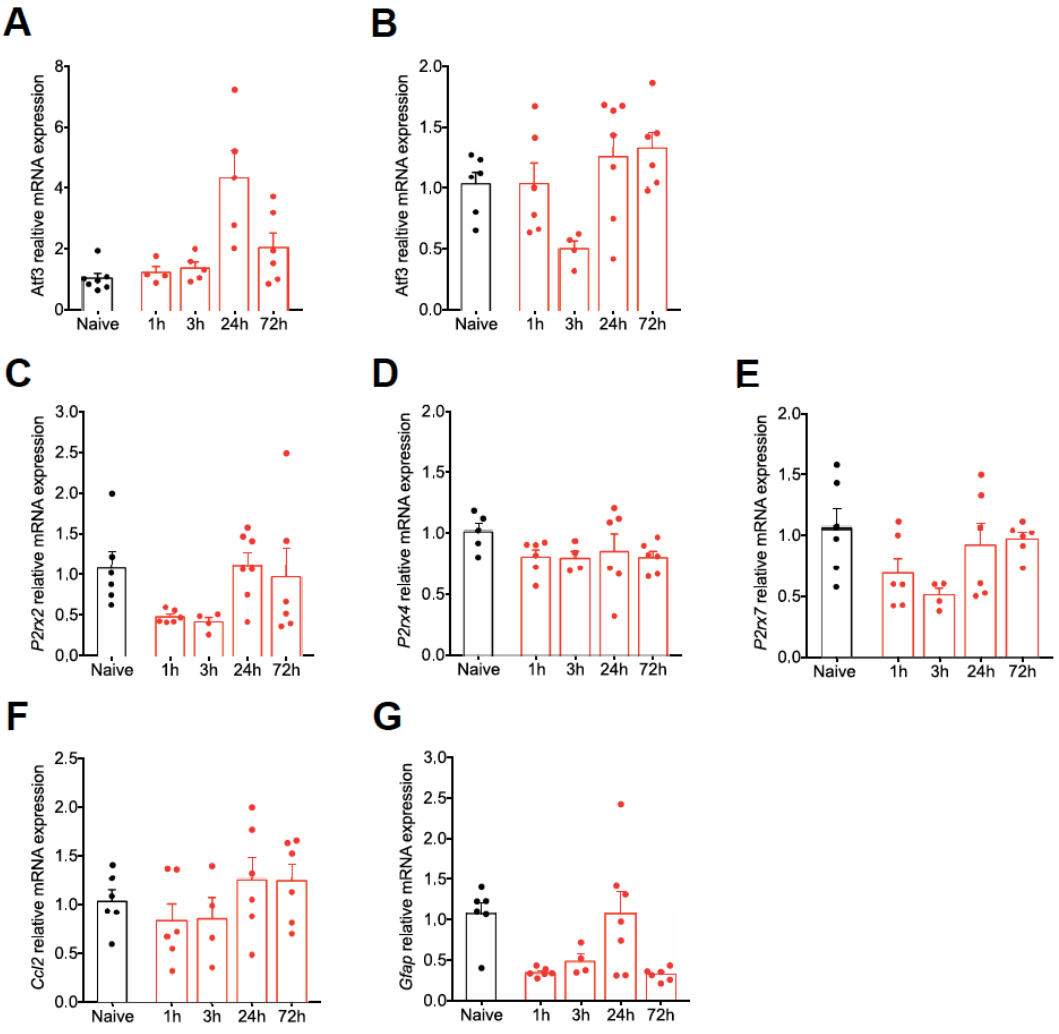

Fig. S7. Expression of nerve injury and inflammatory markers in spinal cord of mice subjected to incisional wound

(A and B) mRNA expression (relative to GAPDH) of ATF-3, a neuronal death marker, in the DRGs (A) and spinal cord (B) of mice after incisional wound. (C-G) mRNA expression (relative to GAPDH) of glial activation markers (P2X2/4/7, CCL2, and GFAP) in the spinal cord of mice after incisional wound. Data are represented as mean±SEM; all data analyzed using one-way ANOVA with *post-hoc* Bonferroni test (*P<0.05, **P<0.01, and ***P<0.001). Data are representative of at least n=2 experiments.

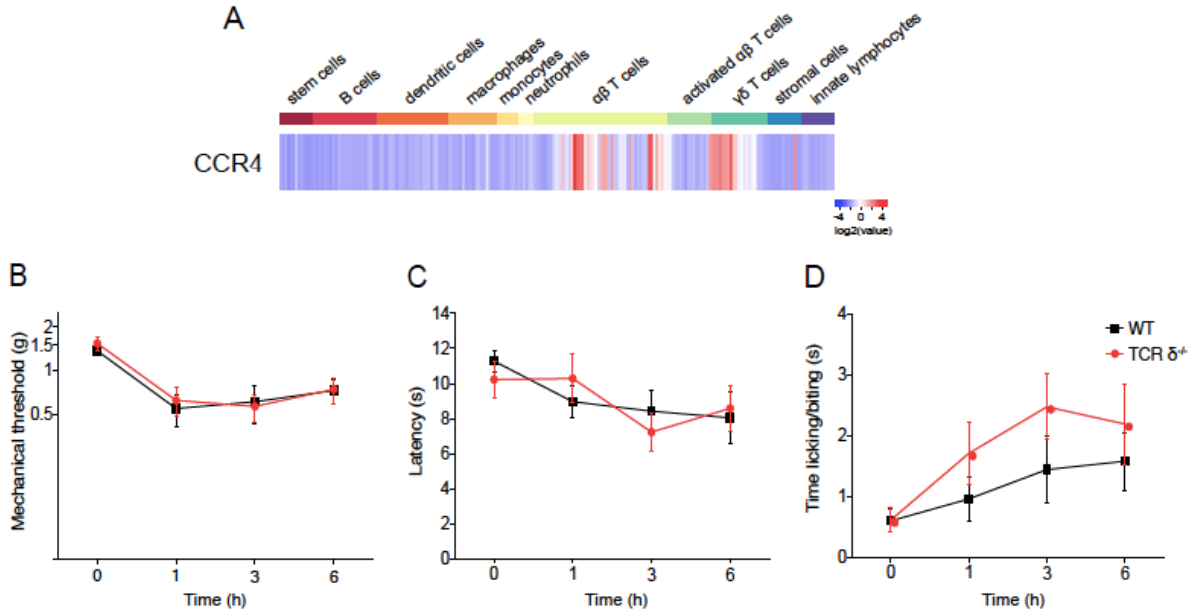

Fig. S8. γδ T cells do not contribute to the generation via CCL17 and CCL22.
(A) Expression profiling of CCR4 among key immune cell populations using the ImmGen database. (B-D) TCRδ$^{-/-}$ and wildtype littermates received intraplantar injections with 30nM of both CCL17 and CCL22 (n=10/genotype). No differences were observed between the genotypes in mechanical (B), thermal heat (C), or cold (D) hypersensitivity in the first 6 hours after injection. Data is represented as mean±SEM; all data analyzed using two-way ANOVA with *post-hoc* Bonferroni test (*P<0.05, **P<0.01, and ***P<0.001). Data are representative of at least n=2 experiments.

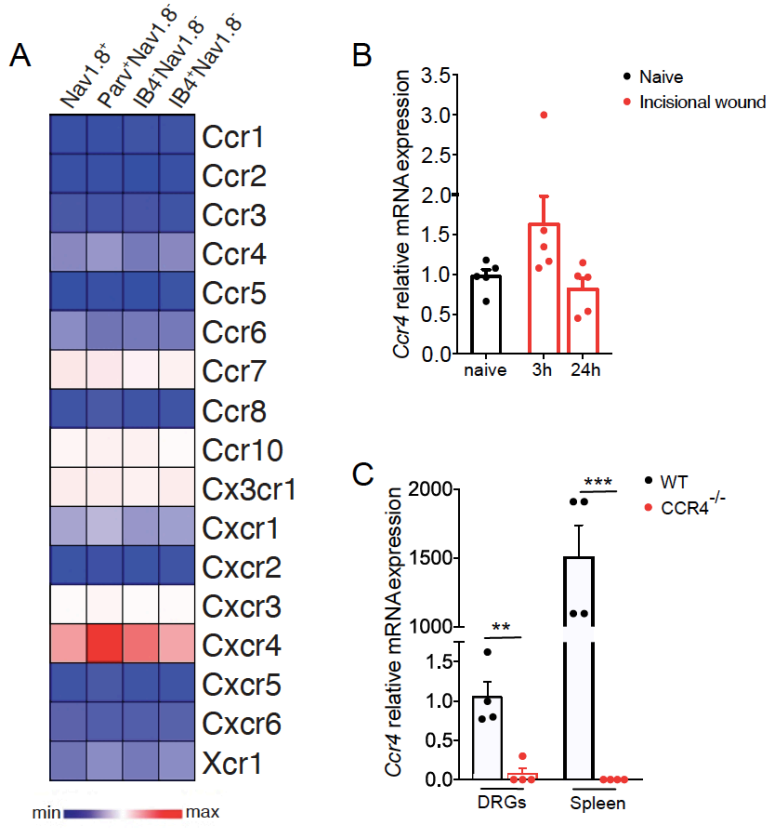

Fig. S9. CCR4 is expressed in DRG neurons.

(A) Expression of all chemokine receptor genes shows that CCR4 is expressed by peripheral sensory neurons. (B) Changes in mRNA expression of CCR4 (relative to GAPDH) in the DRG of C57BL/6 mice after incisional wound were assessed over the course of injury (n=5/timepoint). A slightly increase was observed at 3h but it returned to basal levels at 24h. (C) CCR4 mRNA expression (relative to GAPDH) is abolished in $CCR4^{-/-}$ mice, compared to WT animals. The spleen, used as control, also show complete absence of CCR4 expression. Data are represented as mean±SEM; all data analyzed using one-way ANOVA with *post-hoc* Bonferroni test (*P<0.05, **P<0.01, and ***P<0.001). Data are representative of at least n=2 experiments.

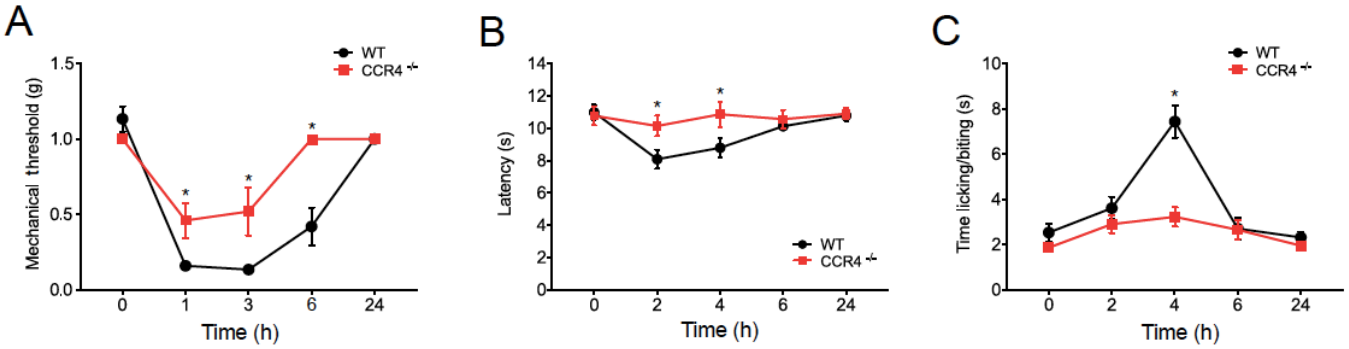

Fig. S10. CCR4$^{-/-}$ mice are resistant to pain hypersensitivity caused by CCL22. Male CCR4$^{-/-}$ mice received an intraplantar injection of CL22 (n=10/group) at 30 nM; saline was used as a control. (A) Changes in mechanical hypersensitivity, measured using von Frey monofilaments, show that CCL22 does not cause reductions in threshold in CCR4$^{-/-}$ mice. (B) Thermal heat hypersensitivity, measured using the Hargreaves radiant heat test, shows that thermal pain induced by CCL22 is inhibited in CCR4$^{-/-}$mice. (C) Similarly, cold hypersensitivity, assessed using the acetone test, is greatly reduced in CCR4$^{-/-}$ mice. Data is represented as mean±SEM; all data analyzed using two-way ANOVA with *post-hoc* Bonferroni test (*P<0.05, **P<0.01, and ***P<0.001 vs. saline-treated controls). Data are representative of at least n=2 experiments.

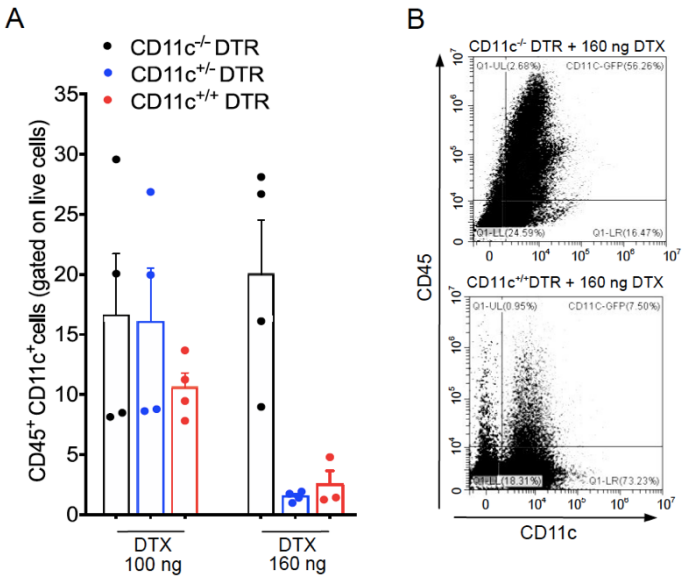

Fig. S11. Optimization of DTX treatment and CD11c$^+$ cell depletion.

(A,B) CD11c-DTR mice (all genotypes) were treated with 100ng or 160 ng of DTX through intraperitoneal injection. 24 h after the injection, both paws were collected and processed for flow cytometry. (A) Frequency of CD11c$^+$CD45$^+$ cells on the paw of both groups of treated mice. (B) Representatives dotplots of WT (CD11c$^{-/-}$) and CD11c$^{+/+}$ mice treated with 160ng of DTX.

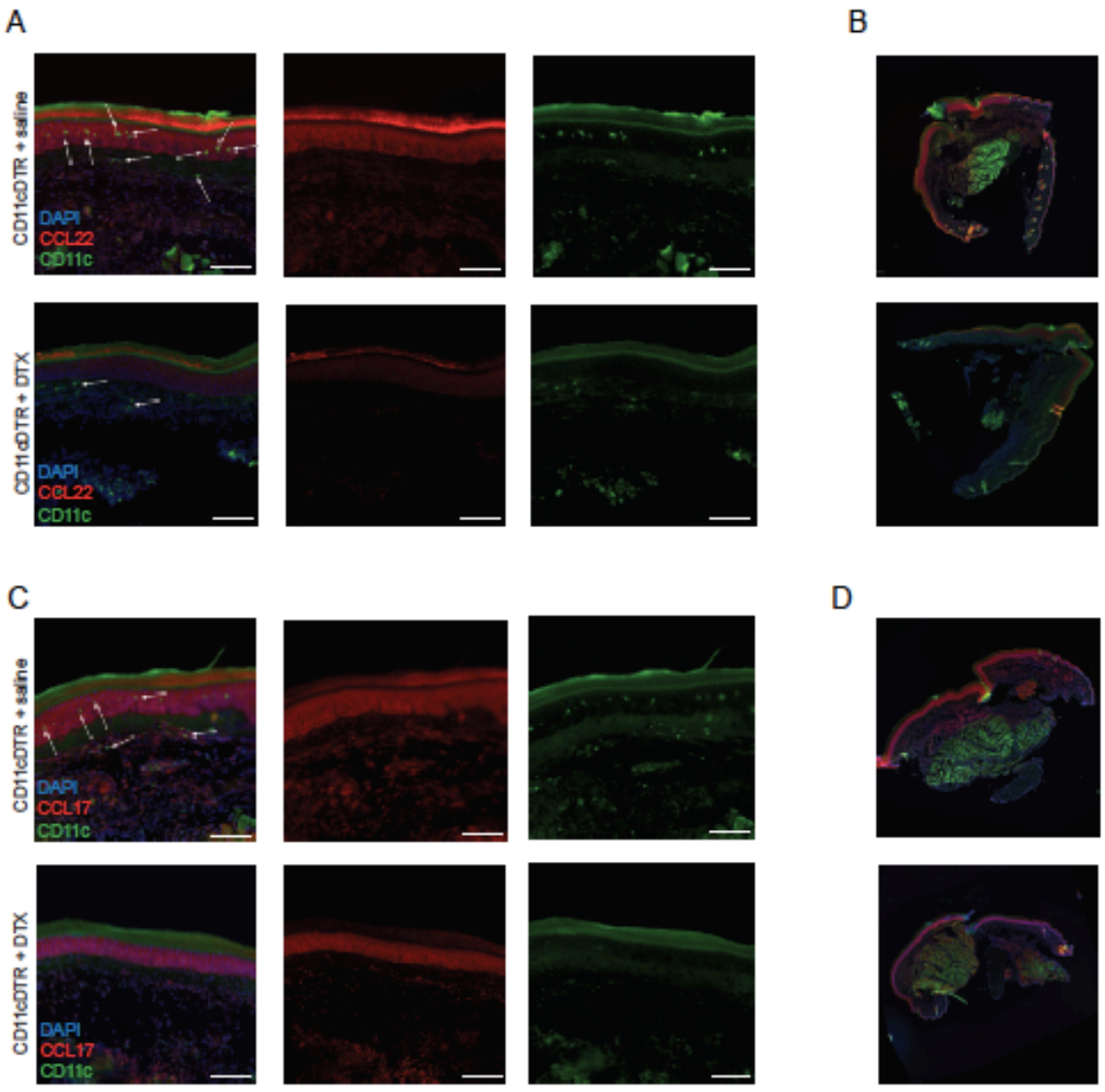

Fig. S12. CCL22 and CCL17 protein expression are reduced after CD11c^{+} cell depletion.

CD11c$^{+/-}$ mice were treated with DTX or saline and incisional wound was performed after CD11c^{+} cell depletion. 24h after surgery the ipsilateral paws were collected and processed for histology. Immunofluorescence analysis of paw sections from both groups of mice revealed the reduction of expression of both CCL22 (A) and CCL17 (C) in CD11^{+} depleted animals not only at the site of injury (A, C), but in the whole paw (B, D). Arrows point to immunopositive cells. Scale bar = 50 μm.

Supplementary text

Materials and Methods

Experimental animals

All work was performed in 6–12-wk-old male mice housed in a light- and temperature-controlled room. C57BL/6J mice (Jackson Labs, stock #000664) were used for all the described experiments. CD11c-DTR/GFP (Jackson Labs, stock #004509) (1), Lang-DTREGFP (Jackson Labs, stock #016940) (2) and CCR4$^{-/-}$ mice (Jackson Labs, stock #004101) (3), all of them on the C57BL/6J mice background, were used for some of the experiments. The mice were housed in the animal care facility of the Queen's School of Medicine and taken to the testing room at least one hour before experiments. Food and water were available *ad libitum*. All behavioral tests were performed between 9:00 AM and 5:00 PM. Animal care and handling procedures were in accordance with the guidelines of the International Association for the Study of Pain (IASP) on the use of animals in pain research.

CD11c+ dendritic cells depletion

Diphteria toxin (Sigma Aldrich) was reconstituted in sterile water (1mg/ml) and then diluted to the working concentration in sterile saline. Mice were randomly assigned to control and experimental groups. The depletion of CD11c+ cells was performed with an intraperitoneal injection of diphtheria toxin at a concentration of 8ng/gbw (aproximately160ng total per mouse).

Incisional wound surgery

Sterile tissue injury-based peripheral inflammation was induced by using a deep plantar incision of the left hind paw. Briefly, mice were anesthetized with 2% (vol/vol) isoflurane (maintained at 1.5% during surgery) and the left hind paw sterilized with 10% (wt/vol) povidone-iodine and 100% ethanol. The skin and underlying muscle were cut along the midline by using a number-11 scalpel from the base of the heel to the first walking pad, and the overlying skin was sutured at two sites using 6-0 sutures (Ethilon); no analgesics were used postoperatively to allow for early assessment of pain outcomes.

CCR4 knockdown in DRGs

The CCR4 (Ambion, Cat #4457298) and control siRNA (Ambion, Cat #4457287) by Thermo Fisher Scientific were mixed to in vivo-jetPEI® by Polyplus to increase the uptake of siRNA by DRGs. The siRNA was dissolved in RNase-free water at the concentration of 1 μg/μl as stock solution, and a total of 3 μg of siRNA targeting CCR4 or non-targeting control siRNA were diluted in a 10 μl solution with 2.62 μL of in vivo-jetPEI® and 5% glucose. The siRNA (3 μg) was intrathecally injected in the space between L4-L5 for 3 consecutive days. A valid spinal puncture and intrathecal delivery of siRNA was confirmed by a reflexive tail flick after needle entry into the subarachnoid space.

Thermal and mechanical behavioral analysis

Mechanical threshold was measured using von Frey monofilaments (Ugo Basile), and defined as the minimum filament weight needed to elicit at least five responses (fast paw

withdrawal, flinching, licking/biting of the stimulated paw) over a total of 10 stimulations to determine the 50% threshold. For the cold hypersensitivity assessment, the plantar area of the left hind paw was exposed to acetone and the mouse was scored on lifting up, biting or licking the paw. The duration of the reaction was measured and analyzed as cumulative reaction time. Mice were habituated for 1h daily in individual compartments for each behavior assay. Three baseline measurements were then taken on separate days for mechanical threshold and thermal latency to response and averaged. One value was taken per mouse for mechanical threshold and an average of three values was taken per mouse for thermal latency at each time point used. All behavioral experiments were carried out using at least two independent cohorts of mice.

RNA extraction and Real-Time PCR

At indicated times post-injury, the skin of the paw and DRGs were collected from mice after euthanasia. The samples were submitted to: (i) Flow Cytometry and Sorting preparation, as previously described, or (ii) the tissues were directly homogenized in 1 mL of QIAzol (Qiagen). Total RNA was extracted using the RNeasy Mini Kit (Qiagen) following the manufacturer's instructions. The purity of total RNA was measured with a spectrophotometer and the wavelength absorption ratio (260/280 nm) was between 1.8 and 2.0 for all preparations. Reverse transcription of total RNA to cDNA was carried out with a reverse transcription reaction (High Capacity, Thermo Fisher). Real-time PCR was performed using primers specific for the mouse genes *Ccl17, Ccl22* and *Ccr4*, and for the mouse housekeeping gene Glyceraldehyde 3-phosphate dehydrogenase (*Gapdh*). Primer pairs for mouse *Ccl17, Ccl22, Ccr4* and *Gapdh,* were as follows:

Ccl17 fwd: 5'- CAGGAAGTTGGTGAGCTGGTATA -3'

Ccl17 rev: 5'- TTGTGTTCGCCTGTAGTG CATA-3'

Ccl22 fwd: 5'- TCTGATGCAGGTCCCTATGGT- 3'

Ccl22 rev: 5'- TTATGGAGT AGCTTCTTC AC- 3'

Ccr4 fwd: 5′-GGAAGGTATCAAGGCATT TGG G-3′

Ccr4 rev: 5′-GTACACGTCCGTCATGGACTT -3′

Gapdh fwd: 5′- CATCTTCTTGTGCAGTGCCA-3′

Gapdh rev: 5′- CGGCCAAATCCGTTCAC-3′

Flow Cytometry

Analysis of immune cell presence was carried out as previously described (4). Briefly, paw tissue was minced and digested in a mixture of 1 mg/mL collagenase A and 2.4 U/mL Dispase II (Roche Applied Sciences) in Hepes-buffered saline solution for 90 min (Gibco). After digestion, cells were triturated by pipette, washed with HBSS, and filtered through a 70-μm mesh, and blocked by using rat anti-CD16/CD32 (Biolegend; 1:100) on ice for 5 min. The cells were then incubated with mixtures of the following antibodies (all from BioLegend; 1:200 unless noted): PE anti–CD11b, APC-Fire anti–Ly6C, PeCy7 anti-Ly6G, APC anti–CD45 and FITC anti-CD11c. Flow cytometry was conducted on a CytoFLEX machine (Beckman and Coulter).

Microarray gene expression analysis

CD45+CD11b+Ly6G− myeloid cells were sorted based on Ly6C expression (low, medium, high), with transcriptomics analysis carried out using the Affymetrix Mouse

Gene ST 2.0 GeneChip, as previously described (5) (GSE73667). Transcripts were filtered for mean expression values >100 in any one population , keyword searches for immune-related transcripts "immun* OR inflamm*" carried out using Excel (Microsoft), and transcripts sorted by variability across the three populations of cells. Transcriptomic data from FACS purified somatosensory neuron subtypes was previously carried out (6) (GSE55114). Analysis of immune cell subsets was carried out using data collected by the Immunological Genome dataset (7) (GSE15907). GenePattern was used to analyze expression level comparison between targets, using hierarchical clustering with Spearman's Rank correlation analysis and a pairwise average-linkage clustering method. All data were then sorted alphabetically (for chemokine receptors) or by subset (for immune cells). Heat maps were generated by using the GenePattern platform (Broad Institute).

Paw immunofluorescence

CD11c-DTR/GFP and Lang-DTREGFP were terminally anesthetized and perfused with saline, followed by 4% paraformaldehyde in 0.1 M phosphate buffer, pH 7.4 (4°C). The paws were removed and postfixed in the same fixative for 2h, which was then replaced overnight with 30% sucrose. Tissues were frozen in Tissue TEK OCT (Fisher Scientific) and serial 14 μm sections collected using a Leica CM1860 cryostat (Leica). All sections were blocked with 1% BSA in 0.1% Triton X-100 for 1h at room temperature and incubated overnight at 4°C with CCL17 (1:500, Bioss) or CCL22 (1:200, Bioss). After washing, AlexaFluo-594 conjugated secondary antibodies (Jackson Immunoresearch) were added for 2h at room temperature. The slides were mounted using Vectashield with

DAPI (Vector Laboratories, Burlingame, CA). Images were captured using an Eclipse Ti2 microscope (Nikon, Tokyo, Japan) and analyzed with NIS-Elements AR (Nikon).

Western blot analysis

DRGs L4-L6 were homogenized in RIPA buffer (Thermo Fisher Scientific) containing 1X protease inhibitor cocktail and 1X phosphatase inhibitor cocktail (both from Thermo Fisher Scientific). Total protein concentrations were determined using the Pierce BCA protein assay kit (Thermo Fisher Scientific). Equal amounts of proteins (30ug) were loaded and separated on 10% SDS–PAGE and then transferred to polyvinylidene fluoride membranes. The membranes were blocked with 5% BSA and incubated with primary antibodies CCR4 (1:400, Abcam cat#47553, overnight at 4°C) or mouse anti β-actin (1:1000, Invitrogen cat#MA515739, 1h at room temperature), followed by incubation with HRP-conjugated secondary antibodies (Jackson ImmunoResearch, 1:10000). Immunodetection was performed using SuperSignal West Femto Chemiluminescent Substrate (Thermo Fisher Scientific). The density of bands was normalized to β-actin and quantified using Image Studio Lite (LI-COR Biosciences).

Electrophysiological measurements

DRG neurons were excised from 6 week old mice at 24 hours post-incision, and enzymatically dissociated in HBSS containing 2 mg/ml collagenase and 4 mg/ml dispase (Invitrogen) for 45 min at 37 °C. DRGs were then rinsed twice in HBSS without Ca2+ and then resuspended in culture medium consisting of Neurobasal medium (Gibco) supplemented with 10 % heat-inactivated fetal bovine serum (HI-FBS), 100 μg/ml

streptomycin, 100 U/ml penicillin, 100 ng/ml Nerve Growth Factor (all from Invitrogen) and 10% B27 (Gibco). Individual neurons were dispersed by trituration through a fire-polished glass Pasteur pipette and cultured overnight at 37 °C with 5% CO2 in 96% humidity on glass coverslips previously treated with 25% Poly-Ornithine and Laminin (both from Sigma) at 37°C for 24 hours.

Current clamp experiments were performed using small diameter mouse DRG neurons at room temperature in a 2 ml bath containing (in mM): 140 NaCl, 5 KCl, 1.5 $CaCl_2$, 2 $MgCl_2$, 10 HEPES and 10 D-glucose (pH 7.4 adjusted with NaOH, and osmolarity 315 mOsm) on the stage of an inverted epi-fluorescence microscope (Olympus IX51). Borosilicate glass (Harvard Apparatus Ltd.) pipettes were pulled and polished to 3-5 MΩ resistance with a DMZ-Universal Puller (Zeitz-Instruments GmbH.). Pipettes were filled with an internal solution containing (in mM): 140.0 KCl, 5.00 NaCl, 1 $CaCl_2$, 1.0 EGTA, 10.0 HEPES, 1.0 $MgCl_2$, 3.0 ATP Na_2 (pH 7.3 adjusted with KOH, 315 mOsm). Recordings were performed using an Axopatch 200B amplifier (Axon Instruments). Current clamp protocols were applied using pClamp 10.5 software (Axon Instruments). Data were filtered at 1 kHz (8-pole Bessel) and digitized at 10 kHz with a Digidata 1440 A converter (Axon Instruments). Average cell capacitance for the DRG neurons was of 12.235 ± 0.89 pF for control and 12.06 ± 0.62 pF for the neurons from postoperative animals. Only the neurons in which the resting membrane potential was more negative than -45 mV were used and only those cells that exhibited a stable voltage control throughout the recording were used for analysis. All the drugs used were diluted in the extracellular buffer, from a stock solution, to achieve final concentrations. All solutions were prepared and used at room temperature (22±2ºC). The number of

spontaneous action potentials (APs) was calculated as the number of APs per second during extracellular buffer application. The number of evoked APs was calculated as APs per second during the first 30 seconds of CCL22 application (10nM).

Statistics

Data are reported as mean ± SEM. Two-way RM-ANOVA was used to compare the groups and doses at the different times (curves) when the responses (nociception) were measured after surgery or treatment. The analyzed factors were the treatments, the time, and the time versus treatment interaction. The normality of data was analyzed by D'Agostino and Pearson test, which confirm the parametric distribution of data. If there was a significant time versus treatment interaction, one-way ANOVA followed by Tukey's t-test was performed for each time. Alternatively, if the responses (e.g., nociception, mRNA expression) were measured only once after the stimulus injection, the differences between responses were evaluated by one-way ANOVA followed by Tukey's t-test (for three or more groups), comparing all pairs of columns. P values less than 0.05 were considered significant. Statistical analysis was performed with Prism 8 (GraphPad) and SigmaPlot 11 (Systat Software) software packages.

For electrophysiology, the data analysis was completed using Clampfit 10.4 (Axon Instruments), and all electrophysiology curves were fitted using Origin 7.0 analysis software (OriginLab). All averaged data are plotted as mean±SEM. Statistical analyses were completed with Origin 7.0 software using unpaired t-tests with the criterion for statistical significance set at $p < 0.01$.

SI References

1. J. S *et al.*, In vivo depletion of CD11c+ dendritic cells abrogates priming of CD8+ T cells by exogenous cell-associated antigens. *Immunity* **17** (2002).
2. A. Kissenpfennig *et al.*, Dynamics and function of Langerhans cells in vivo: dermal dendritic cells colonize lymph node areas distinct from slower migrating Langerhans cells. *Immunity* **22**, 643-654 (2005).
3. Y. Chvatchko *et al.*, A key role for CC chemokine receptor 4 in lipopolysaccharide-induced endotoxic shock. *The Journal of experimental medicine* **191**, 1755-1764 (2000).
4. I. M. Chiu *et al.*, Bacteria activate sensory neurons that modulate pain and inflammation. *Nature* **501**, 52-57 (2013).
5. N. Ghasemlou, I. M. Chiu, J. P. Julien, C. J. Woolf, CD11b+Ly6G- myeloid cells mediate mechanical inflammatory pain hypersensitivity. *Proc Natl Acad Sci U S A* **112**, E6808-6817 (2015).
6. I. M. Chiu *et al.*, Transcriptional profiling at whole population and single cell levels reveals somatosensory neuron molecular diversity. *Elife* **3** (2014).
7. T. S. Heng, M. W. Painter, The Immunological Genome Project: networks of gene expression in immune cells. *Nat Immunol* **9**, 1091-1094 (2008).